Tetrahedron 74 (2018) 3301–3305

Contents lists available at ScienceDirect

Tetrahedron

journal homepage: www.elsevier.com/locate/tet

Direct enolization chemistry of 7-azaindoline amides: A case study of bis(tetrahydrophosphole)-type ligands

Zhao Li, Hidetoshi Noda, Naoya Kumagai*, Masakatsu Shibasaki*

Institute of Microbial Chemistry (BIKAKEN), Tokyo, 3-14-23 Kamiosaki, Shinagawa-ku, Tokyo, 141-0021, Japan

ARTICLE INFO

Article history:
Received 15 February 2018
Received in revised form
27 March 2018
Accepted 29 March 2018
Available online 31 March 2018

Keywords:
Asymmetric catalysis
Enolates
Copper
Aldol reaction
Mannich reaction

ABSTRACT

7-Azaindoline amides are particularly useful in direct enolization chemistry due to their facilitated enolization in soft Lewis acid/Brønsted base cooperative catalysis. The Cu(I) complex of (*R*,*R*)-Ph-BPE, a bis(tetrahydrophosphole)-type chiral bisphosphine ligand, exhibits consistently high catalytic performance and stereoselectivity irrespective of the nature of the α-substituent of the amides. Unexpectedly, however, alkyl-substituted bis(tetrahydrophosphole)-type ligands have substantially inferior catalytic performance. Evaluation of the optimized structures of Cu(I)/amide and Cu(I)/enolate complexes provided clues to dissecting the diverted reaction outcomes.

1. Introduction

Enolates are perhaps the most commonly used C-nucleophiles in synthetic organic chemistry to forge carbon–carbon connectivity and construct more complex molecular architectures. Formation of the C(sp^3)–C(sp^3) bond leads to the emergence of two consecutive stereogenic centers, and hence the precise stereochemical control of which has long been an intensive topic of research.[1] The concept of sustainability has rapidly gained popularity in modern synthetic chemistry,[2] and truly catalytic processes are spotlighted as synthetically useful reactions with a practical level of stereochemical control, including the enolate-driven reaction manifold, e.g., aldol[1,3] and Mannich[4] reactions. In this context, the end of the last century witnessed the advent of integrated catalytic processes, comprising 1) catalytic in situ generation of nucleophilically active enolate species; and 2) stereoselective delivery of the thus-formed enolates to electrophiles, affording the desired enantioenriched products directly from bench-stable substrate sets.[5] This direct catalytic protocol in enolate chemistry eliminated the mandatory use of activating reagents to provide a more sustainable option for these important reactions. Typical obstacles in these reaction settings originate from the initial catalytic enolization process; the difficulty significantly increases as carbonyl-type substrates become more reluctant to form the corresponding enolates. Consequently, readily enolizable carbonyl compounds, e.g., ketones and aldehydes, are used as potential enolate precursors, and carbonyl compounds bearing less acidic α-protons, e.g., esters and amides, are largely neglected in this useful direct enolization chemistry.[6] A recent collection of studies led by Kobayashi et al. demonstrated an effective 'product base' strategy for taming low-acidic latent enolates.[7,8] We have devoted particular attention to amides as potential enolate precursors due to their Lewis basic nature, which enables specific interactions with designed Lewis acidic catalysts. Our systematic studies identified 7-azaindoline amides **1** as privileged amide-type enolate precursors that permit a series of C–C bond-forming reactions in a catalytic and stereoselective fashion (Scheme 1).[9] The utility of **1** is leveraged by the flexible attachment of α-substituents, including heteroatom functionalities, allowing for the catalytic synthesis of an array of functionalized chiral building blocks. Herein we revisited the collection of catalytic asymmetric transformations using **1** as enolate precursors to guide the stereochemical outcomes. Additional screening studies elucidated the exclusive utility of a 2,5-diphenyl-substituted bis(tetrahydrophosphole) type ligand, which was supported by computational analysis.

* Corresponding authors.
E-mail addresses: nkumagai@bikaken.or.jp (N. Kumagai), mshibasankumagai@bikaken.or.jp (M. Shibasaki).

https://doi.org/10.1016/j.tet.2018.03.073
0040-4020/

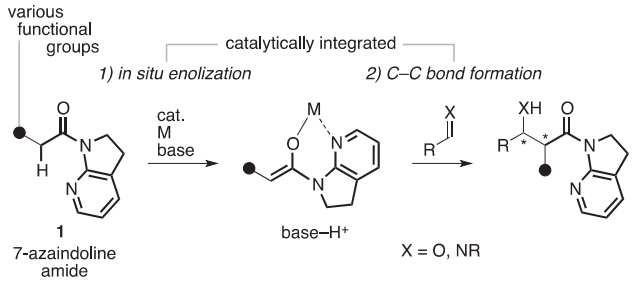

Scheme 1. Structure of 7-azaindoline amides **1** and their utility in direct enolization chemistry.

2. Results and discussion

The proficiency of 7-azaindoline amides **1** is characterized by 1) facilitated enolization as well as 2) a broad compatibility of substituents at the α-position. These amides prefer the *E*-conformation in both solid and solution phase as evidenced by X-ray crystallographic analysis and NMR spectroscopy.[9c] In the presence of protons or Lewis acidic metals, **1** adopts a *Z*-conformation with chelating interactions *via* the pyridyl nitrogen of the flipped 7-azaindoline moiety and the amide oxygen (Scheme 1). This facile chelate formation is likely responsible for subsequent enolization by a catalytic amount of Brønsted base. Typically, Cu(I)/chiral bisphosphine (P-ligand) complex is considered to be an optimal chiral Lewis acid, where Cu(I) is coordinatively saturated. α-Substituents are out of the coordination sphere of Cu(I), and hence various functional substituents are tolerated, e.g., α-alkyl (C),[9f,9g] α-fluoroalkyl (RF),[9b,9c,9h,9i,10] α-azido (N),[9d,9e] α-benzyloxy (O),[9k] α-halo (F, Cl, Br, I),[9j] and α-methylsulfanyl (S),[9a] covering virtually all functional groups used in synthetic organic chemistry. The competent catalyst cocktails are categorized into three variants based on the Brønsted base; A) $[Cu(CH_3CN)_4]PF_6$/P-ligand/Barton's base, B) mesitylcopper/P-ligand, and C) mesitylcopper/P-ligand/phenol derivatives (Fig. 2). Type-A is the most general and intuitive combination with independent functions of the Cu(I)/P-ligand complex and Barton's base as an amide activator and a Brønsted base for deprotonation, respectively. In the case of Type-B, oligomeric mesitylcopper[11] functions as a Brønsted base at the initial catalytic cycle to form a ligated Cu(I)-enolate. Following C–C bond formation with C=O (aldehyde) or C=N (imine) type electrophiles delivers Cu(I)-aldolate or Cu(I)-amide, which functions as a soft Lewis acid/Brønsted base cooperative catalyst[12] for the following catalytic cycle. A mixture of mesitylcopper/P-ligand/phenol derivative leads to a ligated Cu(I)-aryloxide complex in a Type-C catalytic system, analogous to the Type-B catalyst. A series of Cu(I)-catalyzed, aldol, and Mannich-type reactions is illustrated in Fig. 1 based on functional groups at the α-position of the 7-azaindoline amide and classes of P-ligands. This chart reveals that the absolute configuration at the α-position of the carbonyl group is determined by the P-ligand architecture, except for the case of **1-R^F**; (*R*)-biaryls, (*R*,*R*)-Ph-BPE, and (*R*,*R*$_p$)-Walphos prefer α-down, α-up, and α-down configurations, respectively.[13] In contrast, configuration at the β-position is capricious depending on subtle differences in the electrophilic partner. Taken together, the C–C bond formation presumably occurs *via* an acyclic transition state from coordinatively saturated Cu(I)-enolate. (*R*,*R*)-Ph-BPE attracted our particular attention because of its broad utility in the aldol and Mannich-type reactions of **1-N$_3$**, **1-Me**, and **1-Cl** without any screening process using structurally related derivatives. This fact led us to perform the reactions using other BPE derivatives as well as Duphos-type ligands possessing an embedded benzene ring, which share 2,5-disubstituted tetrahydrophosphole units linked by a C2-tether. Table 1 summarizes the aldol or Mannich-type reactions of 7-azaindoline amides and benzaldehyde **3** or aldimine **6** using three BPE-type and two Duphos-type P-ligands. Unexpectedly, alkyl-substituted BPE-type ligands (*R*,*R*)-^{i}Pr-BPE and (*S*,*S*)-Me-BPE[14] were not effective at all in the three reactions shown in Table 1, in marked contrast to the favorable reaction outcomes

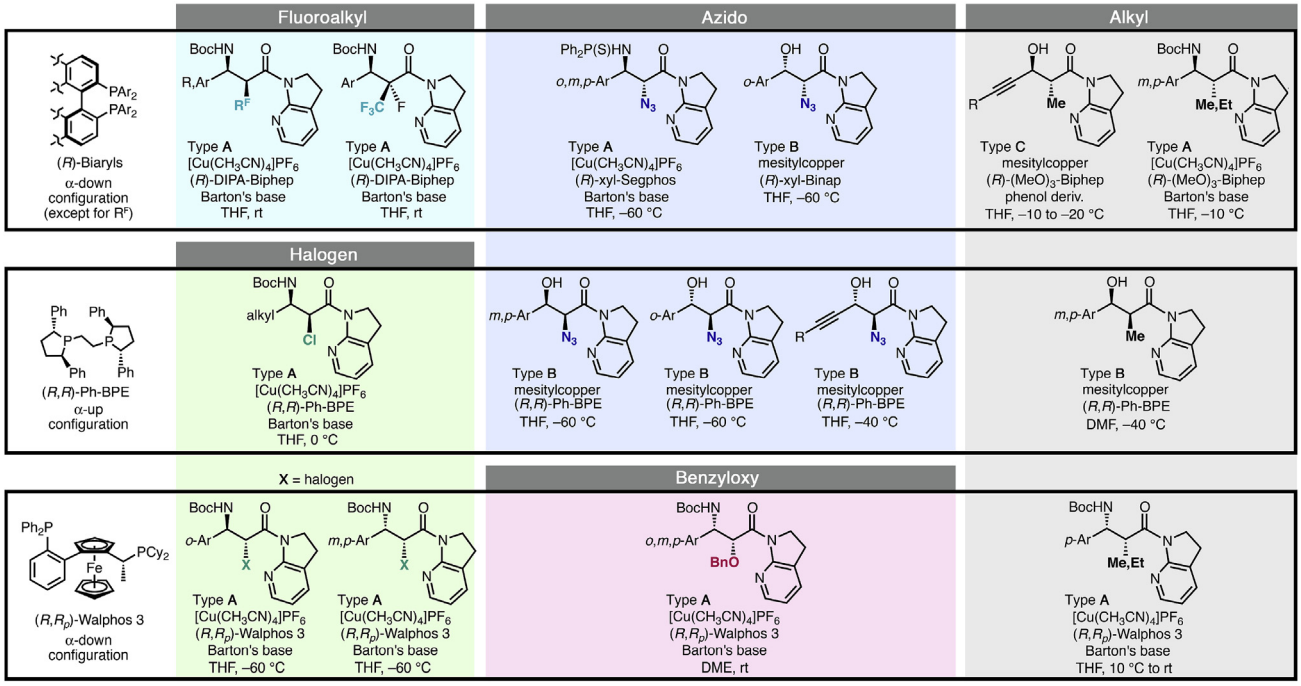

Fig. 1. Schematic representation of Cu(I)/P-ligand catalyzed direct aldol and Mannich reactions. DIPA denotes 3,5-diisopropyl-4-(dimethylamino)phenyl group. Xyl denotes 3,5-dimethylphenyl group.

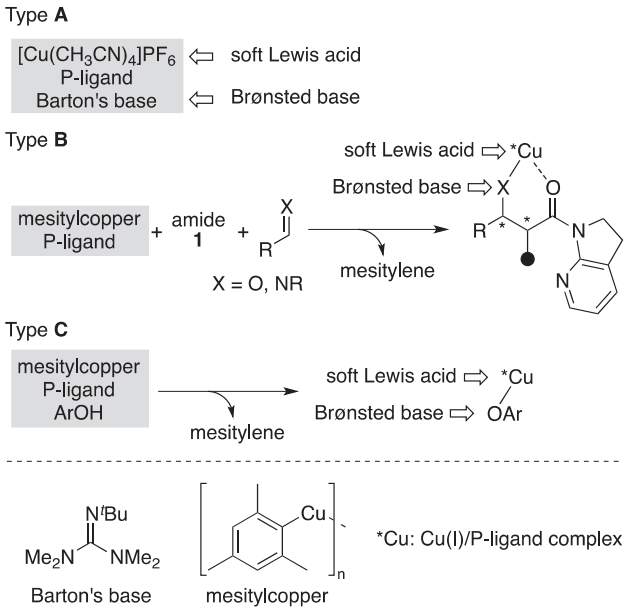

Fig. 2. Three types of soft Lewis acid/Brønsted base cooperative catalysts.

observed with (*R*,*R*)-Ph-BPE. This tendency was consistent with that of the Type-A catalyst for Mannich-type reaction of **1-Cl** and **6**, Type-B catalyst for an aldol reaction of **1-Me**, and Type-C catalyst for an aldol reaction of **1-N$_3$** and **3**. While ^{i}Pr- or Me-substituted Duphos-type ligands performed slightly better than BPE-type counterparts, (*R*,*R*)-Ph-BPE stood out as an outlier in this class of P-ligands. In addition, a comparison of substituents on the identical ligand backbone revealed that smaller Me-substituted P-ligands exhibited worse catalytic activity than ^{i}Pr-analogs.

These experimental outcomes seemed counterintuitive, because the Cu(I) active site of the complexes of Me-substituted P-ligands is more exposed to incoming substrates, and therefore expected to result in a higher reaction rate. To gain insight into the unexpected reaction profiles depending on the substituents of the P-ligands, we modeled the Cu(I)-complexes of (*R*,*R*)-Ph-BPE, (*S*,*S*)-Me-BPE, and (*S*,*S*)-Me-Duphos ligated with amide **1-Me** or the corresponding enolate at the B3LYP/6-31G(d) (SDD for Cu) level of theory using the Gaussian 16 package.[15] Because previous crystallographic analysis of azaindoline amides **1** and the Cu(I)/biaryl-type P-ligand revealed that **1** prefers bidentate coordination to Cu(I) with the conformation of α-substituents proximal to Cu(I),[9c] geometry optimization was performed with similar initial structures and the *Z*-configured enolate. Table 2 summarizes the key structural parameters of these complexes.[16] Differences in bond lengths and bond angles around Cu(I) between the amide and enolate complexes with each ligand were largely corroborative by taking the anionic nature of the enolate into account. The complexes of the three different ligands showed similar structural changes in bond lengths and O–Cu(I)–N_{Py} angle with only marginal deviation, but a significant difference was detected in the change of the O–C_{Am}–N_{Am}–C_{Py} dihedral angle between the amide and enolate complexes. In sharp contrast to the negligible change in the dihedral angle in (*R*,*R*)-Ph-BPE complex (2.593°), a substantially larger magnitude of angular rotation occurred for the (*S*,*S*)-Me-BPE and (*S*,*S*)-Me-Duphos complexes (23.921° and 22.905°, respectively). Considering that in situ enolate generation is typically the rate-limiting step in direct enolization chemistry, the significantly smaller change in the dihedral angle presumably accounts for the facilitated enolization, and hence much faster kinetic profiles were observed for the catalyst with

Table 1
Direct catalytic asymmetric aldol and Mannich-type reactions of **1-N$_3$**, **1-Me**, and **1-Cl** using bis(tetrahydrophosphole)-type chiral P-ligands.[a]

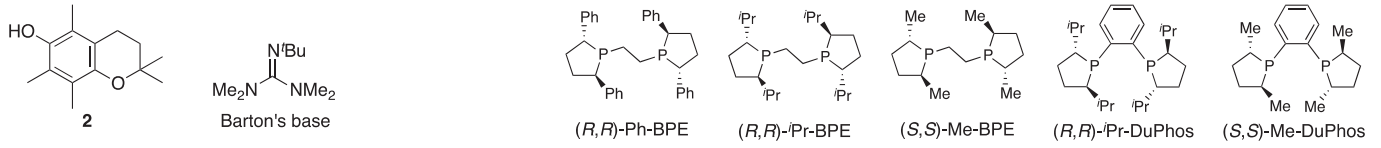

3 + **1-N$_3$**	mesitylcopper P-ligand phenol deriv. **2** 10 mol%[b] THF, –60 °C 24 h Type **C** catalyst	**4**	90% yield[c] *syn*/*anti* = 80/20 95% ee (*syn*)	trace	trace	41% yield[c] *syn*/*anti* = 63/37 73% ee (*syn*)	26% yield[c] *syn*/*anti* = 50/50 8% ee (*syn*)
3 + **1-Me**	mesitylcopper P-ligand 10 mol%[b] DMF, –40 °C 24 h Type **B** catalyst	**5**	82% yield[c] *syn*/*anti* = 82/18 95% ee (*syn*)	trace	trace	trace	trace
6 + **1-Cl**	[Cu(CH$_3$CN)$_4$]PF$_6$ P-ligand Barton's base 10 mol%[b] THF, 0 °C 24 h Type **A** catalyst	**7**	89% yield[c] *syn*/*anti* = 89/11 99% ee (*syn*)	18% yield[c] *syn*/*anti* = 82/18 –6% ee (*syn*)	8% yield[c] *syn*/*anti* = 74/2 62% ee (*syn*)	40% yield[c] *syn*/*anti* = 89/11 85% ee (*syn*)	trace

[a] For **4**: **1-N$_3$**: 0.2 mmol, **3**: 0.24 mmol; For **5**, **1-Me**: 0.1 mmol **3**: 0.15 mmol; For **7**: **1-Cl**: 0.1 mmol, **6**: 0.3 mmol.
[b] 10 mol% each of catalyst components was used for catalyst preparation, except for the reaction using **1-Cl**, where 12 mol% of P-ligand was used.
[c] Determined by ^{1}H NMR analysis using internal standard (3,4,5-trichloropyridine for **5** and **7**, and 1,1,2,2-tetrachloroethane for **4**).

Table 2
Key structural parameters of Cu(I)/P-ligand/amide and Cu(I)/P-ligand/enolate complexes.[a]

	(*R*,*R*)-Ph-BPE		Diff.[b]	(*S*,*S*)-Me-BPE		Diff.[b]	(*S*,*S*)-Me-Duphos		Diff.[b]
	amide complex	enolate complex		amide complex	enolate complex		amide complex	enolate complex	
bond length (Å)									
Cu-O	2.140	2.020		2.139	2.034		2.137	2.020	
Cu-N_{Py}	2.092	2.075		2.096	2.068		2.093	2.074	
O_C_{Am}	1.235	1.296		1.235	1.298		1.235	1.299	
C_{Am}–C_{α}	1.521	1.368		1.522	1.366		1.523	1.365	
bond angle (deg)									
O-Cu-N_{Py}	85.688	89.550		86.099	91.221		85.972	90.626	
dihedral angle (deg)									
O-C_{Am}-N_{Am}-C_{Py}	−6.323	−8.9162	2.593	−1.648	−25.570	23.921	0.879	−23.784	22.905
	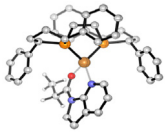	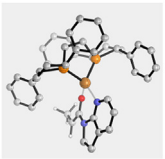		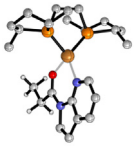	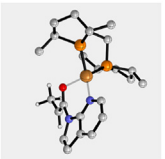		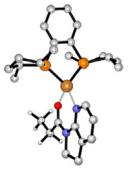	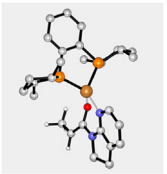	

[a] For optimized structures, protons of ligands and the 7-azaindoline unit are omitted for clarity. Color codes; hydrogen: white, carbon: grey, nitrogen: blue, oxygen: red, phosphorus: orange, copper: brown.
[b] Absolute value of difference between the amide complex and the enolate complex.

(*R*,*R*)-Ph-BPE in direct aldol reactions of 7-azaindoline amides.

3. Conclusion

7-Azaindoline amides are particularly useful pronucleophiles in direct enolization chemistry, allowing for direct aldol and Mannich-type reactions with chiral Cu(I) catalysts in a highly stereoselective manner. Evaluation of a series of reactions revealed that a bis(tetrahydrophosphole)-type P-ligand, (*R*,*R*)-Ph-BPE, is a privileged ligand architecture effective for both aldol and Mannich reactions, and 7-azaindoline amides bearing different α-substituents were tolerated. Intriguingly, (*R*,*R*)-Ph-BPE was an outlier among structurally similar alkyl-substituted counterparts in both catalytic activity and stereochemical control. Optimized structures of Cu(I)/ligand/amide and Cu(I)/ligand/enolate complexes based on DFT calculations implied that the significantly smaller change in the dihedral angle between the enolate plane and the 7-azaindoline unit upon enolization would contribute to the facilitated enolization. In-depth systematic experimental and computational studies of 2,5-diaryl-substituted bis(tetrahydrophosphole)-type ligands are underway.

4. Experimental section

General Experimental Methods. Unless otherwise noted, all reactions were carried out in oven-dried glassware fitted with a three-way glass stopcock under argon atmosphere and stirred with Teflon-coated magnetic stir bars. All workup and purification procedures were carried out with reagent-grade solvents under ambient atmosphere. 7-Azaindoline amides **1-N_3**, **1-Me**, and **1-Cl** were prepared according to the reported procedures.[9e,f,j]

*4.1. (2S,3R)-2-Azido-1-(2,3-dihydro-1H-pyrrolo[2,3-b]pyridin-1-yl)-3-hydroxy-3-phenylpropan-1-one (**4**)*

A flame-dried 20-mL test tube equipped with a magnetic stir bar and a 3-way glass stopcock was charged with amide **1-N_3** (40.6 0.2 mmol), benzaldehyde **3** (25 μL, 0.24 mmol), and 2,2,5,7,8-pentamethyl-6-chromanol **2** (4.4 mg, 0.02 mmol). Dry THF (0.3 mL) was added to the mixture and the test tube was immersed in an electronically-controlled cooling bath at −60 °C. The catalyst solution was prepared as follows and added to the solution. A flame-dried 20-mL test tube equipped with a magnetic stirring bar and a 3-way glass stopcock was charged with (*R*,*R*)-Ph-BPE (10.1 mg, 0.02 mmol) and mesitylcopper (3.7 mg, 0.02 mmol) in a dry box. THF (0.3 mL) was added to the mixture *via* a syringe equipped with a stainless-steel needle at room temperature. A pale yellow solution of (*R*,*R*)-Ph-BPE/mesitylcopper was obtained, which was used within 5 min. After 24 h of stirring at −60 °C, the reaction was quenched with sat. aq. NH_4Cl and the biphasic mixture was extracted with EtOAc. The combined organic layers were washed with brine and dried over Na_2SO_4. After evaporation of the solvent under reduced pressure, the residue was submitted to ^1H NMR analysis to determine the yield and diastereomeric ratio. The enantiomeric excess was determined by HPLC analysis (CHIRALPAK IB (ϕ 0.46 cm × 25 cm), *n*−hexane/2-propanol = 9/1, flow rate 1.0 mL/min, detection at 254 nm, t_R = 28.4 (major), 41.2 (minor).

*4.2. (2S,3S)-1-(2,3-Dihydro-1H-pyrrolo[2,3-b]pyridin-1-yl)-3-hydroxy-2-methyl-3-phenylpropan-1-one (**5**)*

A flame-dried 20-mL test tube equipped with a magnetic stir bar and a 3-way glass stopcock was charged with amide **1-Me** (17.6 mg, 0.1 mmol). Dry DMF (0.15 mL) was added to the mixture and the test tube was immersed into an electronically-controlled cooling

bath at −40 °C. The catalyst solution was prepared as follows and added to the solution. A flame-dried 20-mL test tube equipped with a magnetic stir bar and a 3-way glass stopcock was charged with (*R*,*R*)-Ph-BPE (5.1 mg, 0.01 mmol) and mesitylcopper (1.8 mg, 0.01 mmol) in a glove box. DMF (0.05 mL) was added to the mixture *via* a syringe equipped with a stainless-steel needle at room temperature. A pale-yellow solution of (*R*,*R*)-Ph-BPE/mesitylcopper was obtained, which was used within 5 min. After the addition of benzaldehyde **3** (15 μL, 0.15 mmol) at −40 °C, the mixture was stirred for 24 h at the same temperature. Saturated aq. NH_4Cl was added to quench the reaction and the aqueous layer was extracted three times with EtOAc. The combined organic layers were washed with brine and dried over Na_2SO_4. The filtrate was concentrated under reduced pressure and the residue was submitted to ^1H NMR analysis to determine the yield and diastereomeric ratio. The diastereomeric ratio and enantiomeric excess was determined by HPLC analysis using a CHIRALPAK IF, (Φ 0.46 cm × 25 cm), *n*-hexane/2-propanol = 3/1, flow rate 1.0 mL/min, detection at 254 nm, t_R = 10.8 min (minor), 30.4 min (major).

4.3. *tert*-Butyl((2S,3R)-2-chloro-1-(2,3-dihydro-1H-pyrrolo[2,3-b] pyridin-1-yl)-4-methyl-1-oxopentan-3-yl)carbamate (**7**)

A flame-dried 20-mL test tube equipped with a magnetic stir bar and a 3-way glass stopcock was charged with (*R*,*R*)-Ph-BPE (6.1 mg, 0.012 mmol) and $[Cu(CH_3CN)_4]PF_6$ (3.7 mg, 0.010. mmol, 10 mol%) in a dry box. Anhydrous THF (0.2 mL) was added to the mixture *via* a syringe equipped with a stainless-steel needle at room temperature. The resulting solution was stirred for 1 h and transferred to another test tube prepared as follows: a flame-dried 20-mL test tube equipped with a magnetic stir bar and a 3-way glass stopcock was charged with amide **1-Cl** (19.6 mg, 0.1 mmol) and imine **6** (51.4 mg, 0.3 mmol). The test tube was cooled to 0 °C. Barton's base (0.1 M in THF, 0.1 mL, 0.010 mmol) was added to the mixture *via* a syringe equipped with a stainless-steel needle. After 24 h of stirring at 0 °C, the reaction was quenched with a solution of acetic acid in THF (0.1 M in THF, 1.0 mL). After evaporation of the solvent under reduced pressure, the residue was submitted to ^1H NMR analysis to determine the yield and diastereomeric ratio. The enantiomeric excess was determined by HPLC analysis (CHIRALCEL OD-H (Φ 0.46 cm × 25 cm), *n*-hexane/2-propanol = 19/1, flow rate 0.5 mL/min, detection at 254 nm, t_R = 14.2 min (major), 17.5 min (minor)).

Acknowledgments

This work was financially supported by ACT-C (JPMJCR12YO) from JST, and KAKENHI (17H03025 and JP16H01043 in Precisely Designed Catalysts with Customized Scaffolding) from JSPS.

Appendix A. Supplementary data

Supplementary data related to this article can be found at https://doi.org/10.1016/j.tet.2018.03.073.

References

1. (a) Mahrwald R. *Modern Aldol Reactions*. Weinheim: Wiley-VCH; 2004;
(b) Mahrwald R. *Modern Methods in Stereoselective Aldol Reactions*. Weinheim: Wiley-VCH; 2013.
2. (a) . In: Anastas PT, ed. *Handbook of Green Chemistry*. Weinheim: Wiley- VCH; 2009;
(b) Trost BM. *Science*. 1991;254:1471.
3. (a) Yliniemelå-Sipari SM, Pihko PM. In: Molander GA, ed. *Science of Synthesis: Stereoselective Synthesis*. vol. 2. Stuttgart: Thieme; 2010:621–676;
(b) Alcaide B, Almendros P. *Eur J Org Chem*. 2002:1595;
(c) Notz W, Tanaka F, Barbas III FC. *Acc Chem Res*. 2004;37:580;
(d) Mukherjee S, Yang JW, Hoffmann S, List B. *Chem Rev*. 2007;107:5471;
(e) Trost BM, Brindle CS. *Chem Soc Rev*. 2010;39:1600.
4. (a) Marques MM. *Angew Chem Int Ed*. 2006;45:348;
(b) Ting A, Schaus SE. *Eur J Org Chem*. 2007:5797;
(c) Verkade JM, van Hemert LJ, Quaedflieg PJ, Rutjes FP. *Chem Soc Rev*. 2008;37:29;
(d) Arrayas RG, Carretero JC. *Chem Soc Rev*. 2009;38:1940;
(e) Kobayashi S, Mori Y, Fossey JS, Salter MM. *Chem Rev*. 2011;111:2626.
5. (a) Yamada YMA, Yoshikawa N, Sasai H, Shibasaki M. *Angew Chem, Int Ed Engl*. 1997;36:1871;
(b) Yoshikawa N, Yamada YMA, Das J, Sasai H, Shibasaki M. *J Am Chem Soc*. 1999;121:4168;
(c) List B, Lerner RA, Barbas_III CF. *J Am Chem Soc*. 2000;122:2395;
(d) Trost BM, Ito H. *J Am Chem Soc*. 2000;122:12003.
6. (a) Evans DA, Downey CW, Hubbs JL. *J Am Chem Soc*. 2003;125:8706;
(b) Yamaguchi A, Matsunaga S, Shibasaki M. *J Am Chem Soc*. 2009;131:10842;
(c) Misaki T, Takimoto G, Sugimura T. *J Am Chem Soc*. 2010;132:6286;
(d) Zheng Y, Deng L. *Chem Sci*. 2015;6:6510.
7. Yamashita Y, Kobayashi S. *Chem Eur J*. 2018;24:10.
8. (a) Saito S, Kobayashi S. *J Am Chem Soc*. 2006;128:8704;
(b) Saito S, Tsubogo T, Kobayashi S. *Chem Commun (J Chem Soc Sect D)*. 2007:1236;
(c) Kobayashi S, Kiyohara H, Yamaguchi M. *J Am Chem Soc*. 2011;133:708;
(d) Suzuki H, Sato I, Yamashita Y, Kobayashi S. *J Am Chem Soc*. 2015;137:4336;
(e) Sato I, Suzuki H, Yamashita Y, Kobayashi S. *Organic Chemistry Frontiers*. 2016;3:1241;
(f) Kobayashi S, Yamashita Y, Igarashi R, Suzuki H. *Synlett*. 2017;28:1287.
9. (a) Weidner K, Kumagai N, Shibasaki M. *Angew Chem Int Ed*. 2014;53:6150;
(b) Yin L, Brewitz L, Kumagai N, Shibasaki M. *J Am Chem Soc*. 2014;136:17958;
(c) Brewitz L, Arteaga FA, Yin L, Alagiri K, Kumagai N, Shibasaki M. *J Am Chem Soc*. 2015;137:15929;
(d) Sun Z, Weidner K, Kumagai N, Shibasaki M. *Chem Eur J*. 2015;21:17574;
(e) Weidner K, Sun Z, Kumagai N, Shibasaki M. *Angew Chem Int Ed*. 2015;54:6236;
(f) Arteaga FA, Liu Z, Brewitz L, et al. *Org Lett*. 2016;18:2391;
(g) Liu Z, Takeuchi T, Pluta R, Arteaga Arteaga F, Kumagai N, Shibasaki M. *Org Lett*. 2017;19:710;
(h) Noda H, Amemiya F, Weidner K, Kumagai N, Shibasaki M. *Chem Sci*. 2017;8:3260;
(i) Matsuzawa A, Noda H, Kumagai N, Shibasaki M. *J Org Chem*. 2017;82:8304;
(j) Sun B, Balaji PV, Kumagai N, Shibasaki M. *J Am Chem Soc*. 2017;139:8295;
(k) Sun B, Pluta R, Kumagai N, Shibasaki M. *Org Lett*. 2018;20:526.
10. (a) Brewitz L, Kumagai N, Shibasaki M. *J Fluorine Chem*. 2017;194:1;
(b) Brewitz L, Noda H, Kumagai N, Shibasaki M. *Eur J Org Chem*. 2017:714.
11. (a) Tsuda T, Yazawa T, Watanabe K, Fujii T, Saegusa T. *J Org Chem*. 1981;46:192;
(b) Meyer EM, Gambarotta S, Floriani C, Chiesi-Villa A, Guastinit C. *Organometallics*. 1989;8:1067;
(c) Stollenz M, Meyer F. *Organometallics*. 2012;31:7708.
12. (a) Kanai M, Kato N, Ichikawa E, Shibasaki M. *Synlett*. 2005:1491;
(b) Yamamoto H, Futatsugi K. *Angew Chem Int Ed*. 2005;44:1924;
(c) Paull DH, Abraham CJ, Scerba MT, Alden-Danforth E, Lectka T. *Acc Chem Res*. 2008;41:655;
(d) Yamamoto H, Ishihara K. *Acid Catalysis in Modern Organic Synthesis*. Weinheim: Wiley-VCH; 2008;
(e) Kumagai N, Shibasaki M. *Angew Chem Int Ed*. 2011;50:4760;
(f) Peters R. Weinheim: Wiley-VCH; 2015, 1 online resource.
13. Enantiomeric structures are shown for the examples using (S,S)-Ph-BPE in the literatures.
14. CIP rule labels the methyl-substituted BPE as (S,S), but it bears identical configuration at 2- and 5-positions as (R,R)-Ph- and (R,R)-iPr-BPE.
15. *Gaussian 16, Revision A.03*. Wallingford CT: Gaussian, Inc.; 2016 (See the Supplementary Material for the full citation).
16. Legault CY. *Computed Structures Were Illustrated by Using CYL View. CYLview*. Université de Sherbrooke; 2009, 1.0b http://www.cylview.org/).